

# Multiparametric MRI for early identification of therapeutic response in recurrent glioblastoma treated with immune checkpoint inhibitors

Joseph Song<sup>®</sup>, Priyanka Kadaba, Amanda Kravitz, Adilia Hormigo, Joshua Friedman, Puneet Belani, Constantinos Hadjipanayis, Benjamin M. Ellingson, and Kambiz Nael

*Icahn School of Medicine at Mount Sinai, Department of Radiology (Neuroimaging Advanced and Exploratory Lab), New York, New York (J.S., P.K., A.K., P.B., K.N.); Department of Neurosurgery, Icahn School of Medicine at Mount Sinai, New York, New York (C.H.); Department of Neurology, Medicine (Div Hem Onc), The Tisch Cancer Institute, Icahn School of Medicine at Mount Sinai, New York, New York (J.F., A.H.); UCLA Brain Tumor Imaging Laboratory, Center for Computer Vision and Imaging Biomarkers, Department of Radiological Sciences, David Geffen School of Medicine, University of California Los Angeles, Los Angeles, California (K.N., B.E.)*

**Corresponding Author:** Kambiz Nael, MD, Professor of Radiology, David Geffen School of Medicine at UCLA, 757 Westwood Plaza, Suite 1621, Los Angeles, CA, 90095-7532, Dept. of Radiological Sciences ([Kambiznael@gmail.com](mailto:Kambiznael@gmail.com)).

## Abstract

**Background.** Physiologic changes quantified by diffusion and perfusion MRI have shown utility in predicting treatment response in glioblastoma (GBM) patients treated with cytotoxic therapies. We aimed to investigate whether quantitative changes in diffusion and perfusion after treatment by immune checkpoint inhibitors (ICIs) would determine 6-month progression-free survival (PFS6) in patients with recurrent GBM.

**Methods.** Inclusion criteria for this retrospective study were: (i) diagnosis of recurrent GBM treated with ICIs and (ii) availability of diffusion and perfusion in pre and post ICI MRI (iii) at  $\geq 6$  months follow-up from treatment. After co-registration, mean values of the relative apparent diffusion coefficient (rADC),  $K^{\text{trans}}$  (volume transfer constant),  $V_e$  (extravascular extracellular space volume) and  $V_p$  (plasma volume), and relative cerebral blood volume (rCBV) were calculated from a volume-of-interest of the enhancing tumor. Final assignment of stable/improved versus progressive disease was determined on 6-month follow-up using modified Response Assessment in Neuro-Oncology criteria.

**Results.** Out of 19 patients who met inclusion criteria and follow-up (mean  $\pm$  SD:  $7.8 \pm 1.4$  mo), 12 were determined to have tumor progression, while 7 had treatment response after 6 months of ICI treatment. Only interval change of rADC was suggestive of treatment response. Patients with treatment response (6/7: 86%) had interval increased rADC, while 11/12 (92%) with tumor progression had decreased rADC ( $P = 0.001$ ). Interval change in rCBV,  $K^{\text{trans}}$ ,  $V_p$ , and  $V_e$  were not indicative of treatment response within 6 months.

**Conclusions.** In patients with recurrent GBM, interval change in rADC is promising in assessing treatment response versus progression within the first 6 months following ICI treatment.

## Key Points

- In recurrent GBM treated with ICIs, interval change in rADC suggests early treatment response.
- Interval change in rADC can be used as an imaging biomarker to determine PFS6.
- Interval change in MR perfusion and permeability measures do not suggest ICI treatment response.

## Importance of the Study

Immunotherapy is increasingly used in patients with recurrent GBM, but the interpretation of treatment response versus progression within the first 6 months of treatment is challenging on conventional MR imaging. This study aims to find potential quantitative imaging parameters from MR diffusion and perfusion that can help radiologists

and clinicians recognize and identify treatment-related changes in the early window of post immunotherapy. Early recognition and differentiation of treatment-related response versus progression would be critical in helping neuro-oncologists manage immunotherapy regimens and in determining PFS6 in patients with recurrent GBM.

Glioblastoma (GBM) is the most common malignant primary brain tumor and is associated with poor prognosis and median survival of 18 months.<sup>1</sup> The current standard treatment regime for primary GBM includes a combination of surgical resection, radiotherapy, and chemotherapy including temozolomide (TMZ).<sup>2</sup> Due to the aggressive nature, almost all GBMs recur after initial therapy. Currently the treatment strategy for recurrent GBM remains difficult, since the majority of patients with recurrent GBM do not survive beyond 8 months after diagnosis of recurrent disease.<sup>3,4</sup> While bevacizumab received FDA approval for recurrent GBM, multiple phase II studies did not confirm an overall survival benefit in these patients and therefore other types of treatment are being explored for recurrent GBM.<sup>5</sup>

Most recently, immune checkpoint inhibitors (ICIs) such as programmed cell death 1 (PD-1) inhibitors are being used to treat various solid tumors, including melanoma and non-small-cell lung cancer.<sup>6,7</sup> More recently, the use of ICI in clinical trials for GBM revealed mixed results.<sup>8–11</sup> Treatment with ICIs can lead to T-cell proliferation and production of cytokines with an associated inflammatory response. This inflammatory response can change the blood–brain barrier permeability and result in contrast extravasation and be a major diagnostic challenge on conventional MRI, mimicking imaging appearance of tumor progression with increased enhancement and T2/fluid attenuated inversion recovery (FLAIR) changes, commonly referred to as pseudoprogression.<sup>12</sup> The ambiguities related to interpretation of brain tumor imaging with immunotherapy on conventional brain MRI within the first 6 months of treatment has been acknowledged and reflected in recently updated modified Response Assessment in Neuro-Oncology (RANO) criteria.<sup>13</sup>

In the setting of cytotoxic treatment, advanced MR imaging has been used successfully for early detection of posttreatment changes of pseudoprogression from progressive disease due to pathophysiological differences that can be targeted by use of diffusion and perfusion MRI respectively.<sup>14–18</sup> For example, by probing microscopic motion of water using MR diffusion, diffusion-derived apparent diffusion coefficient (ADC) values inversely correlate with tumor cellular density and can be used for differentiation of treatment-related changes from recurrent tumor.<sup>14,15</sup> Cerebral blood volume (CBV) derived from dynamic-susceptibility contrast-enhanced (DSC) perfusion provide information on neoangiogenesis and microvascular density and can be used for assessment of treatment response.<sup>16,17</sup> Permeability measures such as  $K^{trans}$  (volume transfer constant),  $V_e$  (extravascular extracellular space volume), and  $V_p$

(plasma volume) derived from dynamic contrast-enhanced (DCE) perfusion have been correlated with microvascular leakiness and vascular density and used to differentiate treatment response with some success.<sup>18,19</sup>

There are, however, limited studies examining the potential diagnostic role of MR diffusion and perfusion in recurrent GBM patients treated with ICIs.<sup>20,21</sup> In this study we aimed to identify whether early quantitative changes in diffusion and perfusion MRI before and after ICIs can determine radiographic response at 6 months in patients with recurrent GBM. In particular, we assessed whether interval changes of rADC, rCBV,  $K^{trans}$ ,  $V_e$ , and  $V_p$  obtained from pre-ICI MRI and first post-ICI MRI can be used for early detection of radiographic response or progression at 6 months via modified RANO criteria.

## Materials and Methods

### Patients

This retrospective study was approved by an institutional review board and informed consent was waived. Patients with initial diagnosis of GBM who underwent standard treatment (surgery, fractionated radiotherapy with concurrent and adjuvant TMZ) between July 2014 and July 2018 were reviewed. Patients were then included if (i) they had recurrent GBM (by surgical pathology or by meeting the definition of recurrent disease using RANO criteria) and were treated with ICIs, (ii) had MR diffusion and perfusion before and after ICI treatment, and (iii) had follow-up MRI at 6 months (or beyond) from the ICI treatment for determination of radiographic response.

### Treatment

Patients underwent treatment with ICIs using the standard dose (240 mg of nivolumab every 2 weeks or 200 mg of pembrolizumab every 3 weeks). The number of treatment cycles between pre- and posttreatment MRI was recorded for each patient. Five patients were treated with bevacizumab before the start of ICIs and remained on it throughout the entire period of study follow-up.

### Image Acquisition

All studies were performed on a 3.0T 60 cm bore MR scanner (Discovery MR750, GE Healthcare) using an

8-channel head coil for signal reception. The imaging protocol included a transverse T1-weighted image (repetition time/echo time [TR/TE], 600/82; flip angle [FA], 180°), a T2-weighted image (TR/TE, 7000/100; FA, 180°), and FLAIR (TR/TE, 9000/81; inversion time, 2500 ms), gradient-recalled echo (TR/TE, 870/20; FA, 20°), diffusion, and DCE and DSC perfusion imaging.

Diffusion MR was acquired using single-shot spin-echo echo planar imaging (TR/TE, 4025/82) with  $b$  values of 0 and 1000 s/mm<sup>2</sup>. DCE perfusion was performed using a 3D spoiled gradient recalled echo (GRE) sequence (TR/TE, 4.1/1.8; FA, 10°) with temporal resolution of 7 seconds over a 3.5-minute acquisition time. T1-weighted images with similar acquisition parameters and differing FAs (eg, FAs of 2°, 5°, and 12°) were used for the creation of T1 maps.<sup>22</sup> DSC perfusion was performed using a single-shot gradient-echo echo planar imaging sequence (TR/TE/FA, 1650/30/FA) over a 90-second acquisition time. A single total dose of gadobenate dimeglumine contrast medium (0.1 mmol/kg of body weight) was used for both DCE and DSC perfusion imaging, with 40% of the contrast volume used for DCE imaging and the remaining 60% of contrast volume injected for DSC perfusion. During an 8-minute interval between DCE and DSC, axial T2-weighted and T1-weighted contrast-enhanced images were obtained. The DCE contrast injection was used as a preload for DSC imaging.<sup>23</sup> All injections were performed using an electronic power injector at 5 mL/s, and each contrast injection was flushed with 20 mL of normal saline administered at the same rate.

## Image Analysis

Three MRIs for each patient were included in the study, including (i) pre-ICI treatment (baseline), (ii) post-ICI treatment scan, and (iii) last available follow-up MRI at 6 months (or beyond) from the date of treatment.

All perfusion analyses were performed using commercially available FDA approved software (Olea Sphere, vSP 3.6). Pre-contrast T1 maps were estimated using multiple FA images using previously described methods.<sup>22</sup> DCE perfusion data were post-processed using the extended Tofts model<sup>24</sup> in conjunction with pre-contrast T1 maps to estimate  $K^{trans}$  (volume transfer constant),  $V_e$  (extravascular extracellular space volume), and  $V_p$  (plasma volume) generated.

DSC perfusion estimates of CBV were subsequently post-processed using the Bayesian probabilistic method.<sup>25</sup> For DSC-derived CBV, in addition to contrast preloading, leakage correction was also performed by gamma-variate curve fitting.<sup>26</sup> Parameter maps of ADC, CBV,  $K^{trans}$ ,  $V_e$ , and  $V_p$  for each patient were co-registered with enhanced T1-weighted images by use of a transformation of 6 degrees of freedom and a mutual information cost function.

A volume of interest (VOI) from the enhancing lesion on contrast-enhanced T1-weighted images was generated using a voxel-based signal intensity threshold method subsuming the entire region of enhancement using Olea software. Using co-registered images, mean values of the ADC,  $K^{trans}$ ,  $V_p$ ,  $V_e$ , and CBV were calculated from the VOI of the enhancing tumor in pre-ICI and first post-ICI scans. The CBV and ADC values were normalized to a region of interest placed in normal appearing white matter in the contralateral centrum semiovale (rCBV and rADC).

## Radiographic Response Assessment Using Modified RANO

In patients who were able to tolerate treatment and had available imaging data, radiographic response at 6 months was evaluated according to the updated modified RANO criteria.<sup>13</sup> Lesions were categorized by a board-certified neuroradiologist and a board-certified neuro-oncologist using imaging and clinical information in conjunction after 6 months from the initial treatment, allowing any possible immune-related progressive enhancement to subside. Interval increase of  $\geq 40\%$  in the volume of enhancing lesion on the last MRI ( $\geq 6$  mo), development of new lesions, or substantial clinical decline were considered as progressive disease. Lesions that regressed in size or remained stable on last MRI (in comparison to baseline scan) were categorized as treatment response. Pseudoprogression was defined as interval increase in size of enhancing tumor on post-ICI MRI (in comparison to pre-ICI scan) and subsequent decrease to or below baseline size on the follow-up final scan.

## Statistical Analysis

The quantitative values of ADC, CBV,  $K^{trans}$ ,  $V_p$ , and  $V_e$  computed across voxels for each enhancing tumor were presented as mean (SD) for normal distribution and as median (interquartile range) for data with non-gaussian distribution. Demographic characteristics and neuroimaging variables, including pre- and post-ICI treatment values of rADC,  $K^{trans}$ ,  $V_p$ ,  $V_e$ , and rCBV were compared between subjects with treatment response and progressive disease using univariate analysis including Fisher's exact test for categorical variables and the unpaired two-tailed  $t$ -test or Mann-Whitney  $U$ -test for continuous variables when appropriate. Multiple comparison Tukey adjusted  $P$ -values were reported.

In addition, the mean values of rADC,  $K^{trans}$ ,  $V_p$ ,  $V_e$ , and rCBV on pre- and post-ICI scans were scored to assess the fit with expected treatment response pattern using an interval change  $\geq 1$  SD.<sup>27</sup> The following designation was applied:

1. For rADC, an interval decrease of greater than or equal to 1 SD was considered an unfavorable pattern (suggestive of progression). Any other pattern was considered favorable and suggestive of relative stability.
2. For  $K^{trans}$ ,  $V_p$ ,  $V_e$ , and rCBV: an interval increase of  $\geq 1$  SD was considered an unfavorable pattern (suggestive of progression). Any other pattern was considered favorable and suggestive of relative stability. The patterns of interval change of these imaging variables between pre- and post-ICI scans were assessed for diagnostic correlation using Fisher's exact test among patients with treatment response and progressive disease.  $P < 0.05$  was used to indicate statistical significance.

## Results

Among 38 patients eligible for this study, a total of 19 (12M, 7F, mean age  $61.4 \pm 10.4$ ) met inclusion criteria. Nineteen patients were excluded due to lack of perfusion and

permeability in pre- or posttreatment MRIs ( $n = 12$ ) or lack of at least 6 months follow-up ( $n = 7$ ) (Fig. 1). The mean interval time between the pre- and post-ICI MRI studies was  $2.7 \pm 1.0$  months. In 4 patients (21%), the second MRIs (post-ICI) with inclusion of perfusion and permeability imaging were obtained between 3 and 4 months following the treatment date. The number of treatment cycles between first and second MRIs were 3, 2–4 (median, interquartile range). The total follow-up time calculated as the time interval between baseline MRI and the last MRI was  $7.8 \pm 1.4$  months (mean  $\pm$  SD). The means  $\pm$  SDs of enhancing tumor volume were  $8.1 \pm 14.7$  mL and  $8.2 \pm 9$  mL in pre- and post-ICI scans and  $11.6 \pm 12.3$  mL in final 6-months follow-up MRI.

Using the last MRI at 6 months (or beyond) and clinical information, 12 patients (63.2 %) were determined to have progression and 7 patients (36.8 %) remained stable or showed decrease in final tumor volume. Five out of 7 patients who had eventual treatment response at 6 months demonstrated pseudoprogression on post-ICI MRI (defined as interval increase in volume of enhancing mass following treatment in comparison to pre-ICI scan and interval decrease volume in the final follow-up imaging). The quantitative values of imaging biomarkers including rADC,  $K^{trans}$ , Vp, Ve, and rCBV in pre- and post-ICI MRI scans are summarized in Table 1. Among all imaging parameters assessed, only posttreatment rADC values were significantly higher ( $P = 0.004$ ) in the treatment response group compared with group with progressive disease (Table 1).

In the assessment of interval change in imaging parameters, only interval change of rADC was suggestive of treatment response ( $P = 0.001$ ). Eleven out of 12 (92%) patients with final diagnosis of progression had unfavorable pattern of rADC change (defined as interval decrease of  $\geq 1$  SD) between pre- and post-ICI scans, while 6/7 patients (86%) with final diagnosis of treatment response had favorable pattern of rADC change following ICI treatment. Due

to potential confounding effect of bevacizumab on ADC values, we performed a subset analysis after removing the 5 patients (who received bevacizumab) and redid Fisher's exact test among the remaining 14 patients. In this subset analysis, 6/7 patients with treatment response had a favorable ADC pattern and 6/7 with progression had an unfavorable pattern of ADC change, resulting in a  $P$ -value of 0.029.

Figure 2 shows the plots of percent interval change of rADC and tumor volume over time. Interval change in rCBV and permeability measures, including  $K^{trans}$ , Vp, and Ve, were not suggestive of treatment response (Table 2). In patients with pseudoprogression ( $n = 5$ ), interval increase of rADC (ie, favorable response) was noted in 4/5 (80%), interval decrease in rCBV (ie, favorable response) was noted in 3/5 (60%), interval decrease in  $K^{trans}$  was noted in 4/5 (80%), interval decrease in Ve was noted in 3/5 (60%), and interval decrease in Vp was noted in 4/5 (80%). Figures 3 and 4 show examples of treatment response and progressive disease respectively.

## Discussion

Ongoing advances in cancer immunotherapy challenge physicians and radiologists in image interpretation of treatment response or progression beyond their conventional approach used for cytotoxic cancer therapy. PD-1 inhibitors are one of the currently approved immunotherapy agents that are being explored for treatment of patients with GBM.<sup>28–32</sup> By disrupting the PD-1 pathway, they can incite cytotoxic T cell-mediated tumor destruction<sup>33</sup> and produce significant treatment-related autoimmune and inflammatory reaction within the tumoral bed that can be misinterpreted as disease progression leading to premature termination of therapy.<sup>12</sup> For standard treatment of

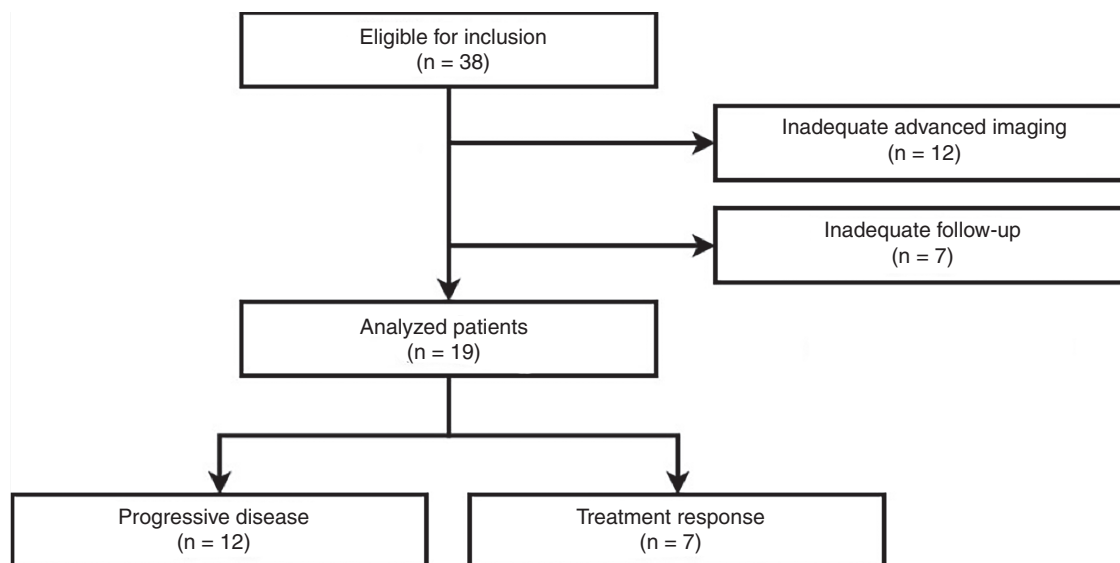


Fig. 1 Study flow diagram showing numbers of included and excluded patients.



**Table 1** Clinical and imaging data in patients with treatment response and progressive disease at 6 months

		Progressive Disease ( <i>n</i> = 12)	Treatment Response ( <i>n</i> = 7)	Univariate Analysis ( <i>P</i> -value)
Age, y		63.4 (9.9)	57.8 (11.1)	0.81
Sex		6 F / 6 M	1 F / 6 M	0.12
Lesion volume, mL	Pre-Tx	8.96 (17.56)	6.72 (8.72)	0.44
	Post-Tx	7.50 (9.41)	9.54 (8.73)	0.76
rADC	Pre-Tx	1.87 (0.42)	1.77 (0.29)	0.37
	Post-Tx	1.65 (0.33)	2.28 (0.92)	<b>0.004</b>
rCBV	Pre-Tx	2.16 (0.93)	1.67 (0.40)	0.25
	Post-Tx	2.20 (1.62)	1.90 (0.65)	0.89
*K <sup>trans</sup> , min <sup>-1</sup>	Pre-Tx	0.08 (0.05–0.13)	0.10 (0.07–0.13)	0.73
	Post-Tx	0.06 (0.04–0.10)	0.08 (0.06–0.16)	0.18
Ve	Pre-Tx	0.26 (0.11)	0.32 (0.18)	0.44
	Post-Tx	0.24 (0.16)	0.32 (0.15)	0.31
*Vp	Pre-Tx	0.05 (0.04–0.08)	0.06 (0.05–0.09)	0.52
	Post-Tx	0.04 (0.03–0.08)	0.04 (0.04–0.13)	0.47

**Abbreviation:** Tx, treatment. Unless otherwise indicated, data are given as mean (SD).

\* Due to non-gaussian distribution, K<sup>trans</sup> and Vp values are presented as median with interquartile range.

GBM with concurrent radiation and cytotoxic treatment (TMZ), RANO criteria have been used for determination of treatment response assessment. Progressive enhancement within the tumoral bed should not be assigned as progressive disease within the first 3 months following completion of cytotoxic treatment as it may represent pseudoprogression according to RANO criteria.

Immunotherapy-related pseudoprogression and treatment-response patterns can be delayed in comparison to cytotoxic treatment, and sometimes reduction in tumor burden may take up to 6 months in patients with proper treatment response.<sup>34,35</sup> Recognizing these complexities, immunotherapy RANO criteria have expanded the window of pseudoprogression to 6 months, justified by the predictable delay for the stimulation of an immune response suggesting close observation with serial imaging within the first 6 months following immunotherapy to properly identify treatment response.<sup>36</sup> After 6 months, new or continued worsening should be deemed tumor progression.

Similar to cytotoxic treatment, imaging of patients with GBM following immunotherapy can be confusing, and conventional imaging has shown mixed results for prediction of treatment-related changes in a series of recently published reports.<sup>37–39</sup> Advanced MR imaging such as MR diffusion and perfusion has been successfully used to determine treatment response in patients with GBM treated with cytotoxic treatment and radiation.<sup>14,40–44</sup> There is, however, a paucity of data on the use of MR diffusion and perfusion for assessment of treatment response following immunotherapy.<sup>20,21,37</sup>

In our study, we found that interval change in rCBV values before and after ICI treatment was not indicative of treatment response. A total of 7 of 12 patients showed expected interval increase of CBV following treatment, while only 3/7 who have responded to treatment showed expected interval decrease in rCBV. This is in contrast to

results of cytotoxic treatment, where interval decrease in CBV as a biomarker of neoangiogenesis and microvascular density has been shown to be associated with cytotoxic treatment response.<sup>41,43,44</sup> Interestingly among 5 patients who had imaging definition of pseudoprogression, 4 showed interval decrease in rCBV following ICI treatment despite having an increase in enhancing tumor size. This is consistent with prior reports indicating that rCBV in contrast-enhancing lesion is usually higher in patients with tumor progression in comparison to patients with immunotherapy-related pseudoprogression.<sup>20,21</sup>

Similarly, we found that interval change in permeability measures including K<sup>trans</sup>, Vp, and Ve before and after ICI treatment were not suggestive of treatment response. This finding is also in contrast to results reported in the literature for successful use of permeability measures as a function of vascular density in determination of cytotoxic treatment response.<sup>41,44,45</sup> We hypothesize that unlike the cytotoxic effect of TMZ which can reduce the vascular density, neoangiogenesis, and permeability of tumors, immune-related response induced by PD-1 inhibition does not impact the tumoral vascular bed in a similar fashion or to the degree that it can be measured by perfusion and permeability imaging.

In our study we found that similar to cytotoxic treatment, treatment response following ICIs can be depicted by interval increase in ADC values. In fact, ADC was the only imaging parameter that changed favorably in 6/7 patients and unfavorably (interval decrease) in 11/12 patients following ICI treatment. MR diffusion can assess microscopic motion of water, and diffusion-derived ADC values inversely correlated with tissue structure and cellularity. Interval increase in ADC therefore has been shown to correlate with treatment response following cytotoxic treatment and radiation.<sup>14,40–42</sup> Our results are similar to those of a prior study by Vrabec et al that showed ADC values are lower

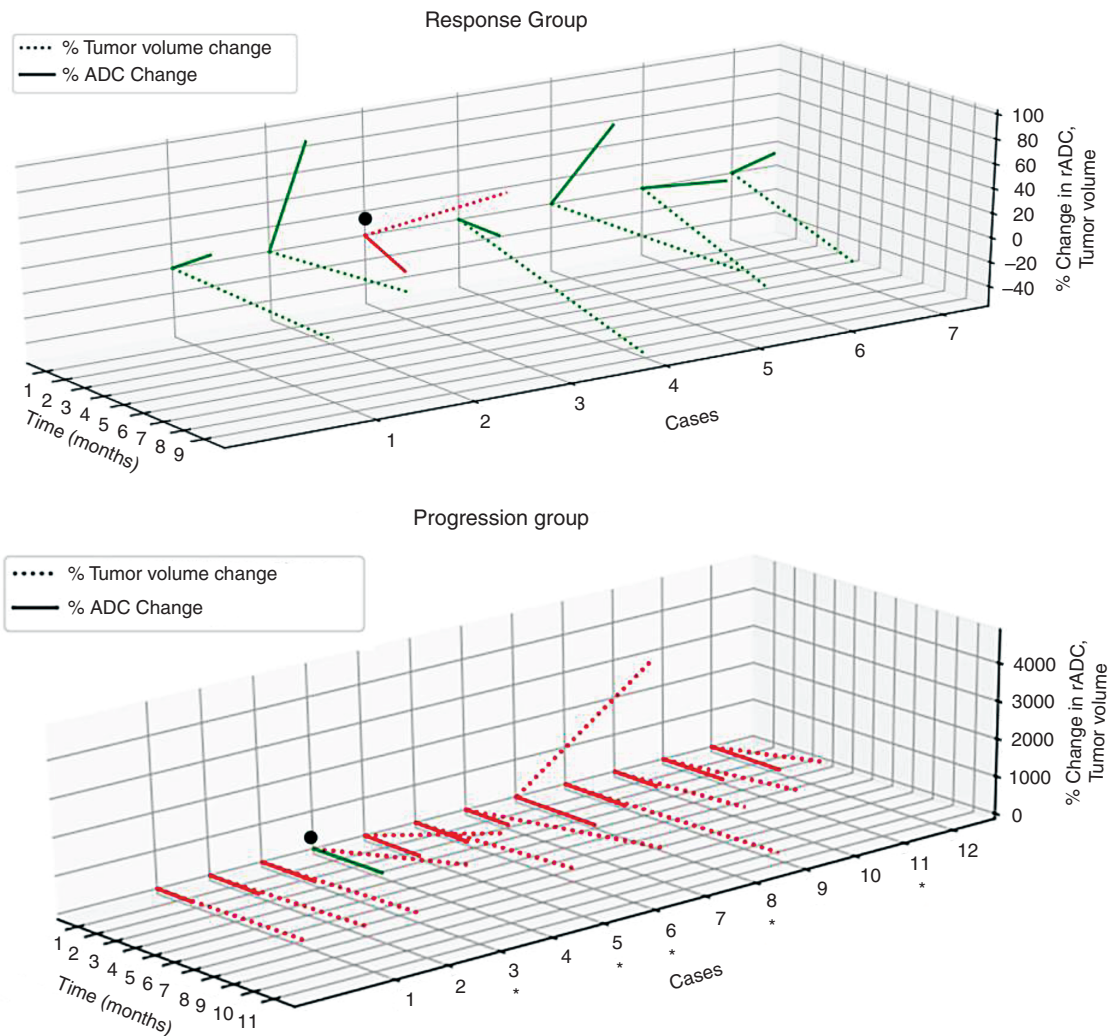


**Fig. 2** Plots demonstrating interval change (%) of rADC and tumor volume over time in patients with treatment response ( $n = 7$ ) and patients with progression ( $n = 12$ ). \*Patients who were treated with bevacizumab during the course of the study. •Patients who didn't show expected interval change of rADC

**Table 2** Sequential rADC, rCBV,  $K^{trans}$ ,  $V_e$ , and  $V_p$  pattern matched with number of lesions in treatment response versus progressive disease at 6 months posttreatment with ICIs

		Progressive Disease ( $n = 12$ )	Treatment Response ( $n = 7$ )	Fisher's Exact Test
rADC	Interval increase	1/12	6/7	<b><math>P = 0.001</math></b>
	Interval decrease	11/12	1/7	
$K^{trans}$	Interval increase	3/12	2/7	$P = 0.90$
	Interval decrease	9/12	5/7	
rCBV	Interval increase	5/12	4/7	$P = 0.32$
	Interval decrease	7/12	3/7	
$V_e$	Interval increase	3/12	4/7	$P = 0.32$
	Interval decrease	9/12	3/7	
$V_p$	Interval increase	3/12	2/7	$P = 0.88$
	Interval decrease	9/12	5/7	

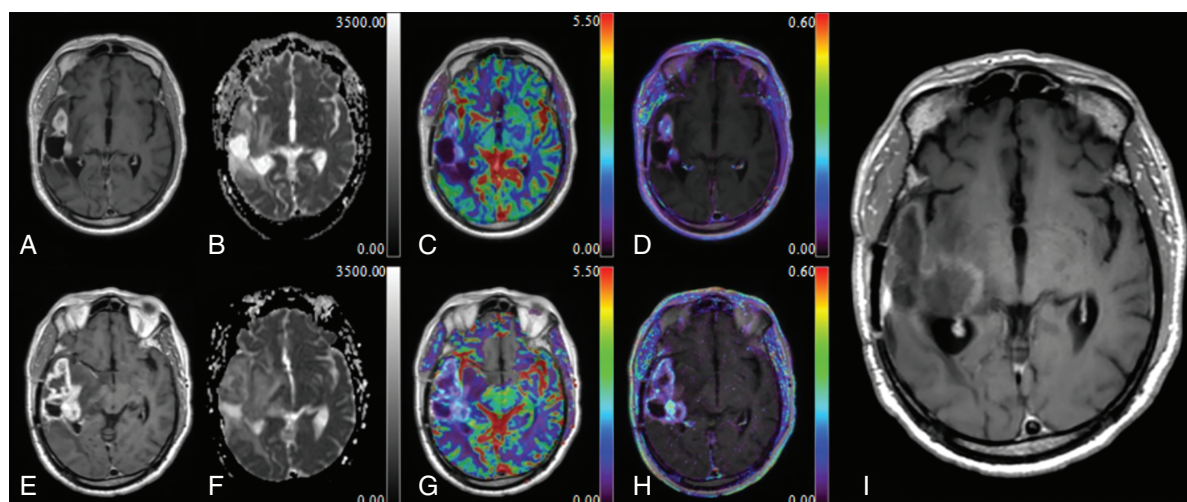


**Fig. 3** A 44-year-old man with recurrent GBM was treated with ICIs. Axial post contrast T1, ADC, CBV, and  $K^{trans}$  maps are shown from pre (top row, A to D) and post (bottom row, E to H)-treatment MRI scans which were obtained 2.4 months apart. There is significant increase in the size of enhancing tissue within and surrounding the tumoral bed on posttreatment MRI. Quantitative analysis of ADC, CBV, and  $K^{trans}$  from the VOI encompassing the enhancing lesion showed: rADC of 2.1/4.3; rCBV of 1.3/1.1 and  $K^{trans}$  of 0.06/0.1 in pre and posttreatment scans respectively. (I) Axial post contrast T1 image from the follow-up MRI obtained 6 months after the initial treatment date shows significant reduction in enhancing tumor burden in this patient who remained clinically stable throughout the course of follow-up.

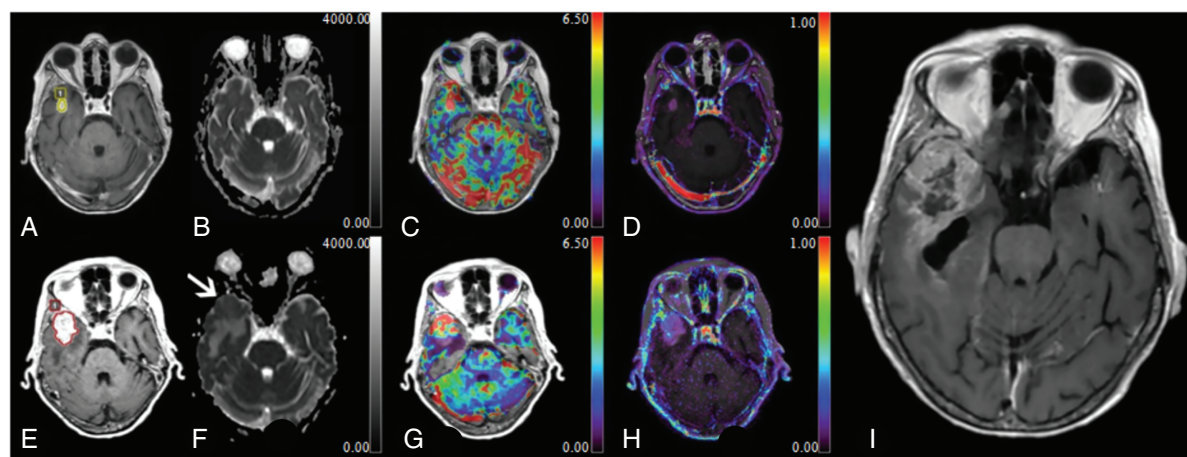


**Fig. 4** A 74-year-old man with recurrent GBM was treated with ICIs. Axial post contrast T1, ADC, CBV, and  $K^{trans}$  maps are shown from pre (top row, A to D) and post (bottom row, E to H)-treatment MRI scans which were obtained 2.3 months apart. There is significant increase in the size of enhancing tissue within and surrounding the tumoral bed on the immediate posttreatment scan. Quantitative analysis of ADC, CBV, and  $K^{trans}$  from the VOI encompassing the enhancing lesion showed: rADC of 2.4/1.5; rCBV of 3.4/5.6 and  $K^{trans}$  of 0.1/0.07 in pre and posttreatment MRIs respectively. (I) Axial post contrast T1 image from the follow-up MRI obtained 6 months after the initial treatment date shows significant increase in enhancing tumor burden in this patient who demonstrated progression throughout the course of follow-up.

in tumor progression compared with stable disease following immunotherapy.<sup>21</sup>

Our study has several limitations. This is a retrospective study, which could introduce unknown bias. Although our study encompasses one of the largest series of patients with recurrent GBM who had pre and post immunotherapy advanced MR imaging, our sample size is still small and a larger study is needed to generalize our imaging findings.

Also since our goal was to assess the role of advanced MRI in determination of PFS6 following immunotherapy, we only included patients who had at least 6 months of follow-up. Therefore, there is a selection bias toward patients who did better and survived longer. The effect and potential diagnostic role of advanced MRI in a group with more aggressive recurrence or less favorable response to immunotherapy is not adequately evaluated with this study. There



is some variability in terms of imaging follow-up in our cohort, which was beyond our control due to retrospective nature. While post-ICI MRIs were obtained approximately 8 weeks following ICI treatment in most patients, in 4 patients MRI with adequate sequences for this study (including perfusion and permeability) were obtained later on. Another limitation of our study is that our analysis does not account for intratumoral heterogeneity. We have no information on PD-ligand 1 (PD-L1) expression in our cohort. There is a wide range of PD-L1 expression in GBM tumors, ranging from 2.8% to 88%.<sup>46,47</sup> This may affect the imaging findings following treatment and the rate of pseudoprogression and progression, although studies in other types of cancer have not always found correlation between PD-L1 expression and response to treatment.<sup>46,48</sup> Five patients were treated with bevacizumab, which could have a confounding effect on quantitative analysis of our imaging biomarkers. However, bevacizumab was started before the immunotherapy in all of these patients (before baseline MR imaging) and therefore the interval change of quantitative imaging parameters should be a reflection of immunotherapy effect.

## Conclusions

In summary, interpretation of treatment response versus progression in recurrent GBM is challenging following immunotherapy. Radiologists should become familiar with potential effects of immunotherapy and recognize different patterns and the wide range of treatment response in these patients as immunotherapy is more widely used in GBM patients. Our study shows that interval change in rADC may prove to be a useful imaging biomarker within the early window of post immunotherapy to recognize and identify treatment-related changes. If its potential is realized, by using interval change in rADC, radiologists could play a critical role in successful management of immune-related toxic effects by differentiating treatment-related response versus progression to reassure both patients and neuro-oncologists to continue with ongoing immunotherapy regimens.

## Keywords

glioblastoma | immunotherapy | MR diffusion | MR perfusion | treatment response

## Funding

None.

**Conflicts of interest statement.** K.N.: Consultant to Olea Medical, None for others.

**Authorship statement.** Study design: AH, KN. Data collection: JS, PK, PB, KN. Statistical analysis: JS, KN. Manuscript preparation: JS, PK, AK, AH, JF, PB, CH, BE, KN.

**Previous presentation.** The preliminary result of this paper was presented at the American Society of Neuroradiology (ASNR), abstract #2993 on 5/22/2019, Boston, MA, USA.

## References

1. Paolillo M, Boselli C, Schinelli S. Glioblastoma under Siege: an overview of current therapeutic strategies. *Brain Sci.* 2018;8(1):15.
2. DeAngelis LM, Wen PY. Primary and metastatic tumors of the nervous system. In: Kasper D, Fauci A, Hauser S, Longo D, Jameson JL, Loscalzo J, eds. *Harrison's Principles of Internal Medicine, 19e.* New York, NY: McGraw-Hill Education; 2014.
3. Lamborn KR, Yung WK, Chang SM, et al; North American Brain Tumor Consortium. Progression-free survival: an important end point in evaluating therapy for recurrent high-grade gliomas. *Neuro Oncol.* 2008;10(2):162–170.
4. Ballman KV, Buckner JC, Brown PD, et al. The relationship between six-month progression-free survival and 12-month overall survival end points for phase II trials in patients with glioblastoma multiforme. *Neuro Oncol.* 2007;9(1):29–38.
5. Cohen MH, Shen YL, Keegan P, Pazdur R. FDA drug approval summary: bevacizumab (Avastin®) as treatment of recurrent glioblastoma multiforme. *Oncol.* 2009; 14(11):1131–1138.
6. Hodi FS, O'Day SJ, McDermott DF, et al. Improved survival with ipilimumab in patients with metastatic melanoma. *N Engl J Med.* 2010;363(8):711–723.
7. Socinski MA. Advances in immuno-oncology: immune checkpoint inhibitors in non-small cell lung cancer-introduction. *Semin Oncol.* 2015;42(Suppl 2):S1–S2.
8. Reardon DA, Freeman G, Wu C, et al. Immunotherapy advances for glioblastoma. *Neuro Oncol.* 2014;16(11):1441–1458.
9. Mantica M, Pritchard A, Lieberman F, Drappatz J. Retrospective study of nivolumab for patients with recurrent high grade gliomas. *J Neurooncol.* 2018;139(3):625–631.
10. McGranahan T, Therkelsen KE, Ahmad S, Nagpal S. Current state of immunotherapy for treatment of glioblastoma. *Curr Treat Options Oncol.* 2019;20(3):24.
11. Reardon DA, Groot JFD, Colman H, et al. Safety of pembrolizumab in combination with bevacizumab in recurrent glioblastoma (rGBM). *J Clin Oncol.* 2016; 34(15\_suppl):2010.
12. Hodi FS, Hwu WJ, Kefford R, et al. Evaluation of immune-related response criteria and RECIST v1.1 in patients with advanced melanoma treated with pembrolizumab. *J Clin Oncol.* 2016;34(13):1510–1517.
13. Ellingson BM, Wen PY, Cloughesy TF. Modified criteria for radiographic response assessment in glioblastoma clinical trials. *Neurotherapeutics.* 2017;14(2):307–320.
14. Chenevert TL, Stegman LD, Taylor JM, et al. Diffusion magnetic resonance imaging: an early surrogate marker of therapeutic efficacy in brain tumors. *J Natl Cancer Inst.* 2000;92(24):2029–2036.
15. Rodriguez Gutierrez D, Manita M, Jaspan T, Dineen RA, Grundy RG, Auer DP. Serial MR diffusion to predict treatment response in high-grade



- pediatric brain tumors: a comparison of regional and voxel-based diffusion change metrics. *Neuro Oncol.* 2013;15(8):981–989.
16. Boxerman JL, Schmainda KM, Zhang Z, Barboriak DP. Dynamic susceptibility contrast MRI measures of relative cerebral blood volume continue to show promise as an early response marker in the setting of bevacizumab treatment. *Neuro Oncol.* 2015;17(11):1538–1539.
  17. Schmainda KM, Prah M, Connelly J, et al. Dynamic-susceptibility contrast agent MRI measures of relative cerebral blood volume predict response to bevacizumab in recurrent high-grade glioma. *Neuro Oncol.* 2014;16(6):880–888.
  18. Jain R. Measurements of tumor vascular leakiness using DCE in brain tumors: clinical applications. *NMR Biomed.* 2013;26(8):1042–1049.
  19. Bisdas S, Naegele T, Ritz R, et al. Distinguishing recurrent high-grade gliomas from radiation injury: a pilot study using dynamic contrast-enhanced MR imaging. *Acad Radiol.* 2011;18(5):575–583.
  20. Stenberg L, Englund E, Wirestam R, Siesjö P, Salford LG, Larsson EM. Dynamic susceptibility contrast-enhanced perfusion magnetic resonance (MR) imaging combined with contrast-enhanced MR imaging in the follow-up of immunogene-treated glioblastoma multiforme. *Acta Radiol.* 2006;47(8):852–861.
  21. Vrabec M, Van Cauter S, Himmelreich U, et al. MR perfusion and diffusion imaging in the follow-up of recurrent glioblastoma treated with dendritic cell immunotherapy: a pilot study. *Neuroradiology.* 2011;53(10):721–731.
  22. Cheng HL, Wright GA. Rapid high-resolution T(1) mapping by variable flip angles: accurate and precise measurements in the presence of radiofrequency field inhomogeneity. *Magn Reson Med.* 2006;55(3):566–574.
  23. Paulson ES, Schmainda KM. Comparison of dynamic susceptibility-weighted contrast-enhanced MR methods: recommendations for measuring relative cerebral blood volume in brain tumors. *Radiology.* 2008;249(2):601–613.
  24. Patlak CS, Blasberg RG. Graphical evaluation of blood-to-brain transfer constants from multiple-time uptake data. Generalizations. *J Cereb Blood Flow Metab.* 1985;5(4):584–590.
  25. Bouteliet T, Kudo K, Pautot F, Sasaki M. Bayesian hemodynamic parameter estimation by bolus tracking perfusion weighted imaging. *IEEE Trans Med Imaging.* 2012;31(7):1381–1395.
  26. Rosen BR, Belliveau JW, Vevea JM, Brady TJ. Perfusion imaging with NMR contrast agents. *Magn Reson Med.* 1990;14(2):249–265.
  27. Knitter JR, Erly WK, Stea BD, et al. Interval change in diffusion and perfusion MRI parameters for the assessment of pseudoprogression in cerebral metastases treated with stereotactic radiation. *AJR Am J Roentgenol.* 2018;211(1):168–175.
  28. Blumenthal DT, Yalon M, Vainer GW, et al. Pembrolizumab: first experience with recurrent primary central nervous system (CNS) tumors. *J Neurooncol.* 2016;129(3):453–460.
  29. Bouffet E, Larouche V, Campbell BB, et al. Immune checkpoint inhibition for hypermutant glioblastoma multiforme resulting from germline biallelic mismatch repair deficiency. *J Clin Oncol.* 2016;34(19):2206–2211.
  30. Cloughesy TF, Mochizuki AY, Orpilla JR, et al. Neoadjuvant anti-PD-1 immunotherapy promotes a survival benefit with intratumoral and systemic immune responses in recurrent glioblastoma. *Nat Med.* 2019;25(3):477–486.
  31. Johanns TM, Miller CA, Dorward IG, et al. Immunogenomics of hypermutated glioblastoma: a patient with germline POLE deficiency treated with checkpoint blockade immunotherapy. *Cancer Discov.* 2016;6(11):1230–1236.
  32. Reardon DA, Omuro A, Brandes AA, et al. OS10.3 randomized phase 3 study evaluating the efficacy and safety of nivolumab vs bevacizumab in patients with recurrent glioblastoma: CheckMate 143. *Neuro Oncol.* 2017; 19(Suppl 3):iii21.
  33. Ribas A. Tumor immunotherapy directed at PD-1. *N Engl J Med.* 2012;366(26):2517–2519.
  34. Pollack IF, Jakacki RI, Butterfield LH, et al. Antigen-specific immune responses and clinical outcome after vaccination with glioma-associated antigen peptides and polyinosinic-polycytidylic acid stabilized by lysine and carboxymethylcellulose in children with newly diagnosed malignant brainstem and nonbrainstem gliomas. *J Clin Oncol.* 2014;32(19):2050–2058.
  35. Kwak JJ, Tirumani SH, Van den Abbeele AD, Koo PJ, Jacene HA. Cancer immunotherapy: imaging assessment of novel treatment response patterns and immune-related adverse events. *Radiographics.* 2015;35(2):424–437.
  36. Okada H, Weller M, Huang R, et al. Immunotherapy response assessment in neuro-oncology: a report of the RANO working group. *Lancet Oncol.* 2015;16(15):e534–e542.
  37. Floeth FW, Wittsack HJ, Engelbrecht V, Weber F. Comparative follow-up of enhancement phenomena with MRI and proton MR spectroscopic imaging after intralesional immunotherapy in glioblastoma—report of two exceptional cases. *Zentralbl Neurochir.* 2002;63(1):23–28.
  38. Ranjan S, Quezado M, Garren N, et al. Clinical decision making in the era of immunotherapy for high grade-glioma: report of four cases. *BMC Cancer.* 2018;18(1):239.
  39. Yang I, Huh NG, Smith ZA, Han SJ, Parsa AT. Distinguishing glioma recurrence from treatment effect after radiochemotherapy and immunotherapy. *Neurosurg Clin N Am.* 2010;21(1):181–186.
  40. Chu HH, Choi SH, Ryoo I, et al. Differentiation of true progression from pseudoprogression in glioblastoma treated with radiation therapy and concomitant temozolomide: comparison study of standard and high-b-value diffusion-weighted imaging. *Radiology.* 2013;269(3):831–840.
  41. Nael K, Bauer AH, Hormigo A, et al. Multiparametric MRI for differentiation of radiation necrosis from recurrent tumor in patients with treated glioblastoma. *AJR Am J Roentgenol.* 2018;210(1):18–23.
  42. Yamasaki F, Kurisu K, Satoh K, et al. Apparent diffusion coefficient of human brain tumors at MR imaging. *Radiology.* 2005;235(3):985–991.
  43. Wesseling P, Ruiter DJ, Burger PC. Angiogenesis in brain tumors: pathobiological and clinical aspects. *J Neurooncol.* 1997;32(3):253–265.
  44. Ly KI, Vakulenko-Lagun B, Emblem KE, et al. Probing tumor micro-environment in patients with newly diagnosed glioblastoma during chemoradiation and adjuvant temozolomide with functional MRI. *Sci Rep.* 2018;8(1):17062.
  45. Tofts PS, Brix G, Buckley DL, et al. Estimating kinetic parameters from dynamic contrast-enhanced T(1)-weighted MRI of a diffusable tracer: standardized quantities and symbols. *J Magn Reson Imaging.* 1999;10(3):223–232.
  46. Nduom EK, Wei J, Yaghi NK, et al. PD-L1 expression and prognostic impact in glioblastoma. *Neuro Oncol.* 2016;18(2):195–205.
  47. Berghoff AS, Kiesel B, Widhalm G, et al. Programmed death ligand 1 expression and tumor-infiltrating lymphocytes in glioblastoma. *Neuro Oncol.* 2015;17(8):1064–1075.
  48. Xue S, Song G, Yu J. The prognostic significance of PD-L1 expression in patients with glioma: a meta-analysis. *Sci Rep.* 2017;7(1):4231.